

**PROCEEDINGS OF THE 16<sup>th</sup> SYMPOSIUM  
ON THE GEOLOGY OF THE BAHAMAS  
AND OTHER CARBONATE REGIONS**

**Edited by  
Bosiljka Glumac and Michael Savarese**

Gerace Research Centre  
San Salvador, Bahamas

2016

Cover photo: San Salvador coastline photo by Erin Rothfus.

Press: A & A Printing

© Copyright 2016 by Gerace Research Centre. All rights Reserved. No part of this publication may be reproduced or transmitted in any form or by any means, electric or mechanical, including photocopy, recording, or any information storage and retrieval system, without permission in written form.

**ISBN 978-0-935909-15-9**

## PROMINENT GEOLOGICAL FEATURES OF CROOKED ISLAND, SE BAHAMAS

Fabienne Godefroid\* and Pascal Kindler

Section of Earth and Environmental Sciences, Maraîchers 13, University of Geneva,  
1205 Geneva, Switzerland

**ABSTRACT.** The most salient geological features observed during a recent reconnaissance trip to Crooked Island, SE Bahamas, include: (1) altered bioclastic calcarenites of probable Early Pleistocene age; and (2) an elevated intertidal notch carved in last interglacial deposits, indicating that sea level peaked at a higher elevation than previously estimated during that time period.

Four main lithostratigraphic units were identified on Crooked Island: (1) highly weathered bioclastic calcarenites that yielded unreliable alloisoleucine/isoleucine (A/I) ratios, and two valid  $^{87}\text{Sr}/^{86}\text{Sr}$  ratios averaging 0.709147; (2) well-lithified bioclastic/peloidal eolianites, forming low sea cliffs, that gave one A/I ratio of 0.523; (3) a complex and extensive unit including scarce coral framestone, exposed up to +1.2 m above sea level, and oolitic-peloidal calcarenites deposited in subtidal, beach, and eolian environments that yielded A/I ratios averaging 0.411 ( $n = 5$ ); and (4) poorly lithified bioclastic beach ridges congruent with modern sea level. Moreover, a prominent ridge along the north coast of the island shows, at +11 m above sea level, an intertidal notch carved in Unit 3 eolianite and filled by Unit 3 beach facies. Units 4, 3 and 2 can be compared, respectively, to the Rice Bay (Holocene), the Grotto Beach (Late Pleistocene) and the Owl's Hole (Middle Pleistocene) formations, previously identified on many other Bahamian islands. Of probable Early Pleistocene age (between 0.6 and 1 Ma), Unit 1 could represent the lowermost part of the Owl's Hole Formation and the top of the underlying, mostly marine Misery Point Formation recently discovered on Mayaguana. The unequivocal occurrence of an intertidal notch carved in, and sealed by, last-interglacial deposits at +11 m shows that the peak elevation reached by sea level during that time interval was much higher than previously assessed. Finally, stratigraphic units decrease in age from N to S, suggesting that the island grew differently than other Bahamian islands or, alternatively, that the northern margin of the Crooked-Acklins bank collapsed in a recent past.

\*Corresponding author. E-mail: Fabienne.Godefroid@unige.ch

### INTRODUCTION

Except for Mayaguana (Godefroid, 2012), the surface geology of the southern Bahamas islands is less well known than that of their northern counterparts such as New Providence (Garrett and Gould, 1984; Hearty and Kindler, 1997; Reid, 2010), San Salvador (Carew and Mylroie, 1985, 1995a; Hearty and Kindler, 1993) or Eleuthera (Hearty, 1998). In particular, there is no published report about the rock exposures on the fairly large islands capping the Crooked-Acklins platform. This paper is a first attempt to bridge this gap in our knowledge. This effort is

justified by the tectonic position of this platform with respect to the North Caribbean plate boundary zone, and by its proximity to Mayaguana where pre-Quaternary rock units have been observed (Kindler et al., 2011; Godefroid, 2012), both of which suggest that the geology of Crooked and Acklins might differ from that of islands located in the northern part of the Bahamian archipelago.

### SETTING

The Crooked/Acklins bank is a medium-size (60 x 85 km) carbonate platform located in

the southeastern part of the Bahamas archipelago (Figure 1). This bank rises from the same 2000 m depth contour as the smaller Mayaguana bank to the East, and is separated from the much larger Great Bahama Bank to the West by the Crooked Island passage (Sealey, 2006). The Crooked/Acklins platform is positioned at about 300 km from the North Caribbean plate boundary zone, but it is in close proximity to the NE extension of the Cauto-Nipe fault, a moderately active, sinistral, strike-slip fault that runs across southern Cuba and through the Mayaguana passage (Figure 1; Cotilla Rodriguez et al., 2007). Despite its location close to an active tectonic zone, the bank is considered to be subsiding slowly due to sediment loading (Lynts, 1970; Carew and Mylroie, 1995b). The triangle-shaped platform bears three main islands (Figure 2): Long Cay, Crooked and Acklins Islands that are located, respectively, along the western, northern and eastern bank margin. These islands enclose an extensive shallow lagoon, the Bight of Acklins that is open to the SW. Crooked Island trends roughly E-W, has a rectangular shape, and is about 40 km long and 10 km wide (Figure 2). As mentioned above, few geologists have investigated the area. Pierson (1982) examined two cores drilled in the central part of the island in the framework of a much larger study. More recently, Rankey and Reeder (2010) investigated the modern sediment distribution and the hydrodynamism of the Bight of Acklins. Finally, a group of geologists lead by J.E. Mylroie explored the prominent karst features of the island (Mylroie, personal communication 2010). Therefore, it seemed timely to undertake a reconnaissance trip to Crooked Island.

## METHODS

This paper stems from five days of fieldwork completed on Crooked Island between February 12<sup>th</sup> and 16<sup>th</sup>, 2011. This investigation included sedimentological and geomorphological

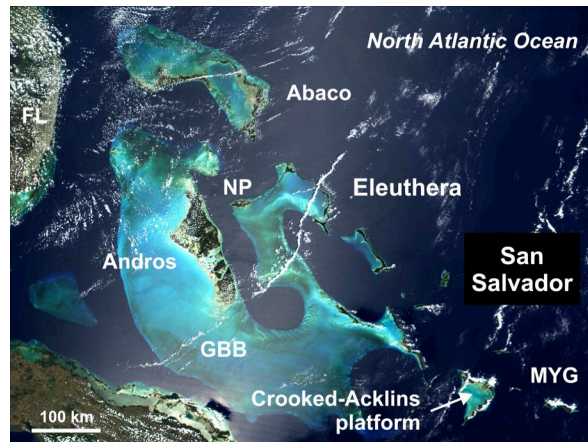


Figure 1. Satellite view of the Bahamas archipelago with the location of the Crooked-Acklins platform. FL = Florida; GBB = Great Bahama Bank; NP = New Providence Island; MYG = Mayaguana Island (image from <http://atlantisbloggen.wordpress.com>).

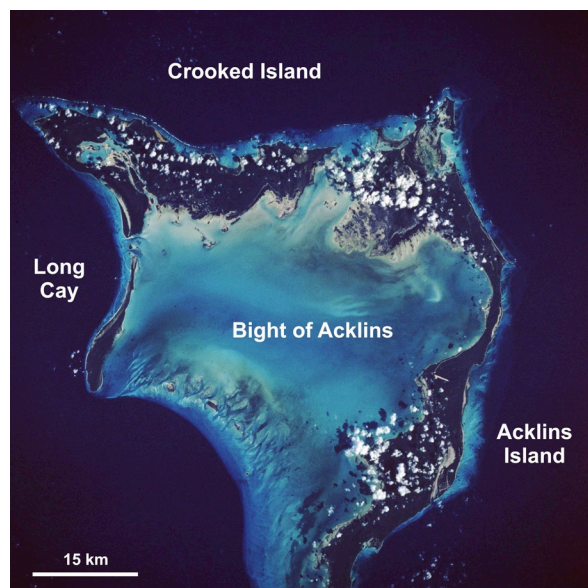


Figure 2. Satellite photo of the Crooked-Acklins platform (image downloaded from <http://earth.jsc.nasa.gov/sseop/images/ReefBase/>).

examination of exposed rock bodies, stratigraphic logging of 17 outcrops (Table 1), and swift geological mapping (Figure 3). Twenty-eight samples were collected for petrographic studies with a transmitted-light microscope. Critical whole-rock samples were dated relatively with the

| Sites # | Locality            | Latitude    | Longitude   |
|---------|---------------------|-------------|-------------|
| 1a      | E of Davies Point   | N22°44.235' | W74°07.317' |
| 1b      | E of Davies Point   | N22°44.239' | W74°07.451' |
| 1c      | E of Davies Point   | N22°44.218' | W74°07.134' |
| 2a      | McKay's Bluff       | N22°44.239' | W74°07.451' |
| 2b      | McKay's Bluff       | N22°45.295' | W74°10.503' |
| 3       | E tip of Crooked    | N22°43.008' | W74°00.730' |
| 4a      | Brown's Settlement  | N22°43.378' | W74°02.339' |
| 4b      | Brown's Settlement  | N22°43.393' | W74°02.399' |
| 4c      | Brown's Settlement  | N22°43.414' | W74°02.527' |
| 5       | Bullet Hill roadcut | N22°44.184' | W74°05.159' |
| 6       | Pitts Town Point    | N22°49.812' | W74°20.961' |
| 7       | Landrail Point      | N22°48.281' | W74°20.436' |
| 8       | Landrail Point      | N22°47.998' | W74°20.240' |
| 9       | Landrail Point      | N22°48.119' | W74°20.320' |
| 10a     | Seaview Settlement  | N22°49.359' | W74°17.263' |
| 10b     | Seaview Settlement  | N22°49.427' | W74°17.235' |
| 11      | Cabbage Hill        | N22°45.959' | W74°12.606' |

Table 1. Geographical coordinates of studied sites.

amino-acid racemization (AAR) and Sr-isotope techniques.

AAR is the interconversion of amino acids from one chiral form (the L -laevo- form) to a mixture of L- and D- (dextro) forms. This chemical reaction is a function of time and

temperature, and can thus be used for geochronology. The extent of the epimerization (i.e., racemization) of L-isoleucine (I) to D-alloisoleucine (A), or A/I ratio, of our selected samples was measured at the Amino Acid Geochronology Laboratory of Northern Arizona University by Prof. D. Kaufmann and his associates. The A/I ratio amounts to zero in modern sediments, and increases to an equilibrium value of 1.3 for infinite-age rocks (Hearty and Kaufman, 2000; 2009). The application of the AAR-dating method to whole-rock samples is discussed in more detail in Hearty et al. (1992) and Hearty and Kaufman (2009).

The <sup>87</sup>Sr/<sup>86</sup>Sr ratio of seawater, and hence of precipitated marine carbonates, varies through time due to changes in continental erosion and oceanic-ridge expansion. The <sup>87</sup>Sr/<sup>86</sup>Sr ratio of pure carbonate sediments of marine origin can thus be used for dating. In this paper, Sr separation and cleaning procedures follow previously published methods (Horwitz et al., 1992).

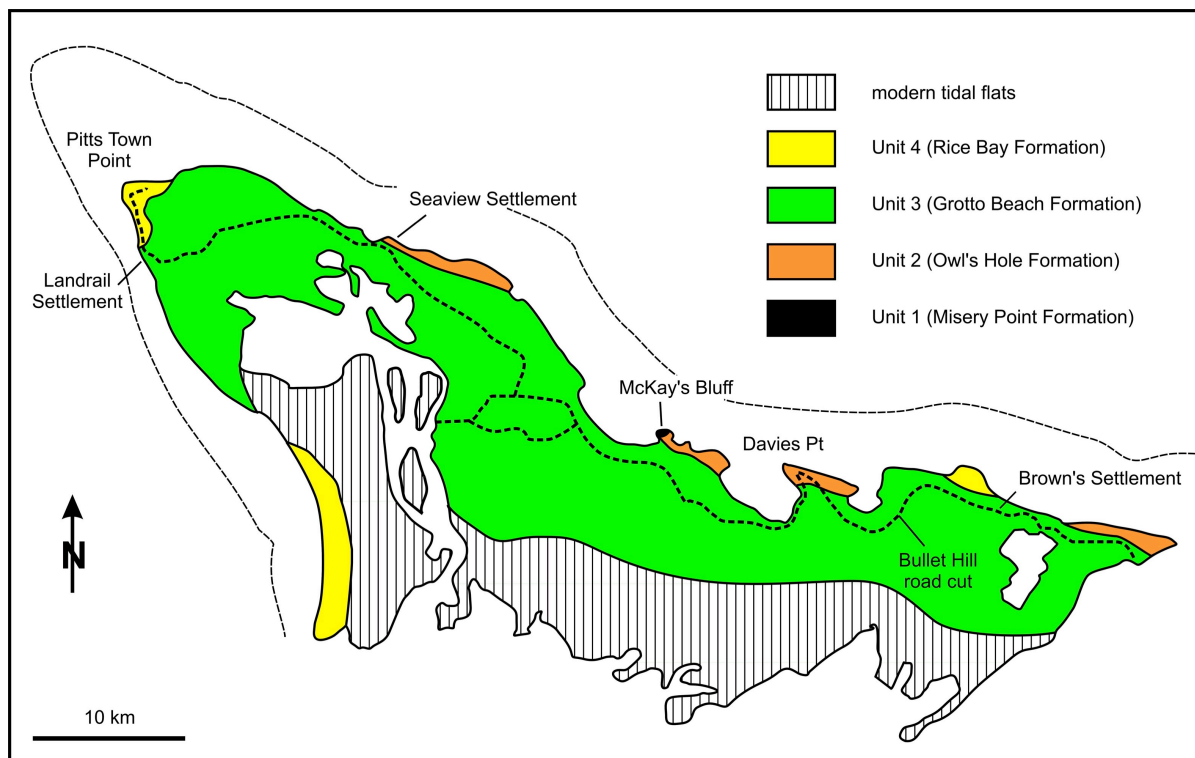


Figure 3. Geological map of Crooked Island compiled during this study. Thin dashed line = bank edge; thick dashed line = paved road.

Measurements were made at the Department of Mineralogy of the University of Geneva by Dr. M. Chiaradia by TIMS in static mode using the virtual amplifier mode. The  $^{87}\text{Sr}/^{86}\text{Sr}$  values were internally corrected for instrumental mass fractionation using an  $^{88}\text{Sr}/^{86}\text{Sr}$  value of 8.375209. All Sr-isotope ratios presented in this study were further corrected for external fractionation by normalization to the given value of the SRM987 standard ( $^{87}\text{Sr}/^{86}\text{Sr} = 0.710248$ ). The external reproducibility ( $2\sigma$ ) of the SRM987 standard was <7 ppm. Numerical ages were then obtained by comparison with the Sr-isotope evolution of global seawater for the Neogene reported as the look-up table Version 4:08/04 (Howarth and McArthur, 1997; McArthur et al. 2001).

## RESULTS

### *Stratigraphy of Crooked Island*

Four major stratigraphic units crop out on Crooked Island. They will be described from the youngest to the oldest (i.e., from Unit 4 to Unit 1).

**Unit 4.** This unit is not very extensive. The best and most accessible outcrops occur along the west coast of the island, to the south of Pitts Town Point (Figure 3). There, this unit forms a rocky shoreline showing partly dismantled, fenestrae-rich, planar cross-beds with a low-angle seaward dip (Figure 4a). These beds consist of moderately lithified, well-sorted, whitish bioclastic calcarenites. Constituent grains are mostly coral, mollusk and algal fragments that are essentially bound by rare low-Mg calcite meniscus cement (Figure 4b). These beds can be identified as fossil beach deposits. Their elevation is similar to that of modern beach sands suggesting that sea level was at about its present datum when they were deposited. No  $^{14}\text{C}$  dating or amino-acid racemization analyses were performed on samples collected from Unit 4. Nonetheless, the low diagenetic grade of this unit and the lack of a capping calcrete or paleosol (Figure 4), both suggest a correlation with the Hanna Bay Member

of the Rice Bay Formation, which has been dated as Late Holocene elsewhere in the Bahamas where it is usually much more widespread (Carew and Mylroie, 1985, 1995a; Kindler, 1992; Hearty and Kaufman, 2009; Savarese and Hoeflein, 2012).

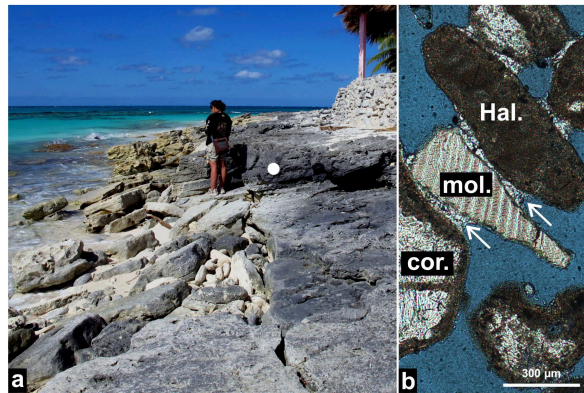


Figure 4. Characteristic features of Unit 4. a) View of the Pitts Town Point exposure showing the partly dismantled seaward-dipping bioclastic calcarenites. Note the absence of a capping calcrete. Person for scale is 1.58 m tall. White dot marks the sampling location of sample CRO23. b) Thin-section view of sample CRO 23 showing various bioclasts cemented by low-Mg calcite menisci (arrows). Note important intergranular porosity; Hal. = Halimeda fragment; mol. = mollusc fragment; cor. = coral fragment.

**Unit 3.** This is the most important stratigraphic unit exposed on Crooked Island (Figure 3). It can be subdivided in two subunits referred to as 3a and 3b.

Subunit 3a is not very extensive. It forms limited exposures of rocky shoreline at Landrail Point Settlement, on the western side of McKay's Bluff (Figure 5a), and to the east of Davies Point. It consists mostly of coral floatstone and rudstone containing dm-sized clasts of *Diploria strigosa*, *Montastrea annularis*, *M. cavernosa*, *Siderastrea* sp. and *Acropora cervicornis* in an oolitic-peloidal grainstone matrix. Coral framestones are scarce on Crooked Island and also comprise the aforementioned species (Figure 5b). These coral-

rich rocks are commonly capped by a cm-thick, brown to red micritic crust (Figure 5a). The maximum elevation at which coral specimens have been observed in life position is +1.2 m above mean sea level (msl). At Landrail Point Settlement, Subunit 3a forms the base of a shallowing-upward succession, the top of which consists of beach beds belonging to Subunit 3b. No dating has thus far been performed on this subunit, but its position below a micritic crust, and the relatively good state of preservation of coral specimens, both suggest a correlation with Marine Isotope Stage (MIS) 5e. This subunit can be further correlated with the Cockburn Town Member of the Grotto Beach Formation (Carew and Mylroie, 1985, 1995a) which forms extensive framestone terraces on neighboring islands (e.g., Great Inagua - Chen et al., 1991; Mayaguana - Godefroid 2012).

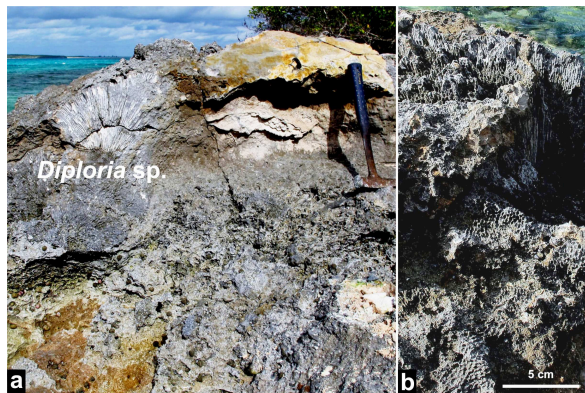


Figure 5. Characteristic features of Unit 3a. a) Coral rudstone/framestone on the western side of McKay's Bluff. Note large *Diploria* head and capping calcrete. Terrace elevation is +1.2 m above sea level. Hammer for scale is 36 cm long. b) Coral framestone with *Montastrea* sp. at the same locality.

Subunit 3b is widely exposed along the coasts (Figure 6a) and in road cuts, and forms the highest ridges on the island (35.4 m -116 feet- at Bullet Hill). It essentially consists of moderately lithified, oolitic-peloidal calcarenites with a wide variety of sedimentary structures (e.g., herringbone cross bedding; fenestrae-rich, low-angle cross bedding; large-scale, steep, landward-

dipping foresets) indicating deposition in diverse peritidal environments (shallow subtidal, Figure 6b; intertidal; supratidal). The high ridges mostly consist of eolian facies. A/I ratios measured on whole-rock samples collected from this subunit yielded an average value of  $0.441 \pm 0.032$  ( $n = 5$ ; Table 2), which corresponds to aminozone E and can be correlated with MIS 5e (Hearty and Kaufman, 2000; 2009). This age is corroborated by the moderate diagenetic grade of these rocks and their position below a micritic crust and/or a *terra-rossa* paleosol. Subunit 3b can be correlated with the French Bay Member of the Grotto Beach

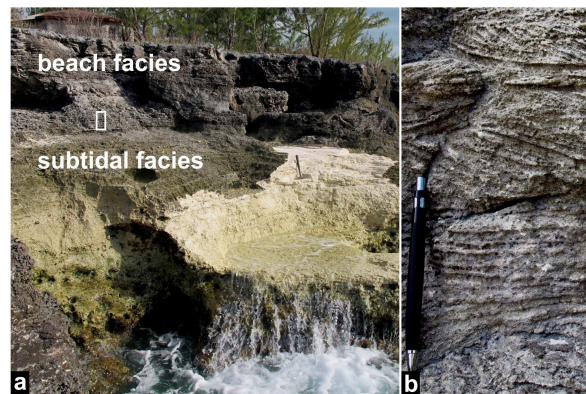


Figure 6. Characteristic features of Unit 3b. a) Coastal exposure near Landrail Settlement showing the subtidal and beach facies. White rectangle shows the position of Figure 6b; hammer for scale is 36 cm long; cliff height is 2.5 m. b) Close-up of Figure 6a showing wave-generated, small-scale, trough cross bedding typical of a subtidal depositional environment. Pen for scale is 15 cm long.

| Sample # | Locality            | Unit | A/I   | Std   | Re |
|----------|---------------------|------|-------|-------|----|
| CRO 10   | Bullet Hill roadcut | 3    | 0.420 | 0.011 |    |
| CRO 11   | Bullet Hill roadcut | 3    | 0.430 | 0.055 |    |
| CRO 12   | Bullet Hill roadcut | 3    | 0.425 | 0.009 |    |
| CRO 13   | Bullet Hill roadcut | 3    | 0.447 | 0.046 |    |
| CRO 17   | McKay's Bluff       | 1    | 0.284 | 0.009 | LC |
| CRO 18   | McKay's Bluff       | 1    | 0.570 | 0.002 | LC |
| CRO 20   | McKay's Bluff       | 1    | 0.569 | 0.075 | LC |
| CRO 21   | McKay's Bluff       | 1    | 0.200 | 0.040 | LC |
| CRO 26   | Seaview Settl.      | 3    | 0.335 | 0.039 |    |
| CRO 27   | Seaview Settl.      | 2    | 0.523 | 0.049 |    |

Table 2. Amino-acid racemization data obtained in this study. A/I = alloisoleucine/isoleucine ratio; Std = standard deviation; Re = remarks; LC = low concentration due to leaching.

Formation (Carew and Mylroie, 1985, 1995a) which is extensively exposed on many Bahamian islands (e.g., Caputo, 1995; Kindler and Hine, 2009; Godefroid, 2012) and is typically composed of oolitic-peloidal grainstone (Kindler and Hearty, 1996).

Unit 2. This unit is well exposed near the ferry dock to Acklins Island and along the north coast near Brown's Settlement and Seaview Settlement (Figure 7a). It consists of moderately to well-lithified calcarenites predominantly composed of bioclasts (Figure 7b). Ooids are scarce in these rocks, but peloids can be fairly abundant. These rocks commonly display large-scale foresets with a steep, landward dip and numerous rhizoliths (root molds, root casts, and rhizocretions). These features, as well as a frequently preserved dune morphology (Figure 7a), indicate deposition in a supratidal (eolian) setting. Unit 2 is always capped by a micritic crust and/or a *terra-rossa* paleosol. Near Seaview Settlement, it occurs below the oolitic facies of the Grotto Beach Formation (Subunit 3b). One A/I ratio measured on the single whole-rock sample gathered from this exposure gave a value of  $0.523 \pm 0.049$  (Table 2), which corresponds to aminozone F/G and suggests a correlation with MIS 7 or 9 (Hearty and Kaufman, 2009). These petrographic and geochronological data, as well as its stratigraphic position suggest that Unit 2 can be correlated with the Owl's Hole Formation (Carew and Mylroie, 1985, 1995a), which is particularly well exposed in Northern Eleuthera (Kindler and Hearty, 1995). Subtle variations in petrographic composition and diagenetic grade between rocks collected from different exposures show that this unit does not represent one single interglacial period of the Middle Pleistocene, but more likely several of these (possibly MIS 9, 11 and 13; Carew and Mylroie, 1995a; Godefroid, 2012).

Unit 1. This unit is only exposed at McKay's Bluff in the central part of Crooked Island (Figures 2 and 3). There, it forms an impressive sea cliff, about 450 m long and over 12

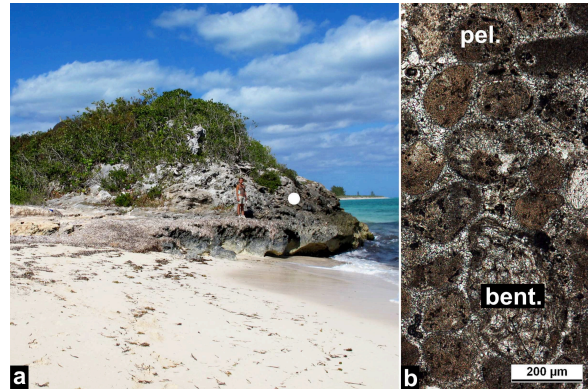


Figure 7. Characteristic features of Unit 2. a) Coastal exposure near Seaview Settlement showing Unit 2 eolianite. Note preserved dune morphology. Person for scale is 1.58 m tall. White dot marks the sampling location of sample CRO27. b) Thin-section view of sample CRO 27 collected from the exposure shown in Figure 7a. Microfacies can be described as a bioclastic-peloidal grainstone. Note widespread sparry cement compared to Figure 4b. bent. = benthic foraminifer fragment; pel. = peloid.

m high (Figure 8a), consisting of extremely altered, coarse-grained bioclastic calcarenites that predominantly contain leached and recrystallized benthic foraminifera and mollusc fragments (Figure 8b). These calcarenites comprise two heavily karstified rock bodies separated and capped by *terra-rossa* paleosols (Figure 8a). The lower one of these rock bodies further encompasses a wave-cut terrace at about +2.5 m above msl (Figure 8a). The upper one shows m-scale foresets with a landward dip (Figure 8a) and can clearly be identified as an eolianite, whereas the lower one is characterized by flatter, undulating, and seemingly multi-directional bedding (Figure 8a). This feature and the occurrence of an early phreatic rim cement in samples collected from the lower part of this unit (Figure 8b) indicate a possible marine origin. Due to leaching, the concentration of amino acids is very low in all analysed samples and obtained values are anomalously small, ranging from 0.200 to 0.570 (Table 2). Hearty (2010) noted that the pattern of increasing A/I ratios with greater age



undergoes a reversal during the early Middle Pleistocene, as amino-acid concentration becomes very low. <sup>87</sup>Sr/<sup>86</sup>Sr ratios obtained from the upper rock body cluster around 0.709147 (Table 3) indicating an Early to Middle Pleistocene age (0.6 to 1 Ma; Gradstein et al., 2004), whereas those measured from the lower unit are unreliable, one of which even yielded a modern age (Table 3). Because it is less evident than in the three previous cases, the stratigraphic attribution of Unit 1 will be addressed in the Discussion section.

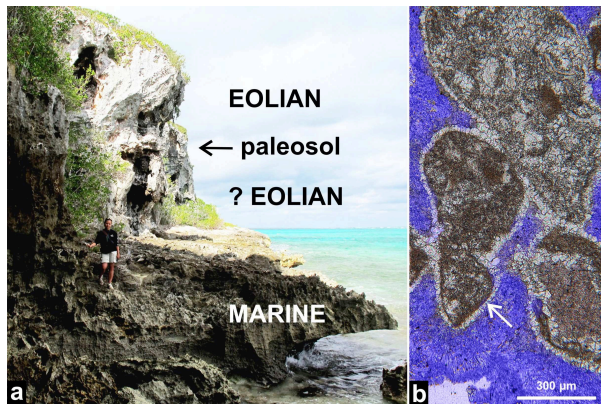


Figure 8. Characteristic features of Unit 1. a) Lateral view of McKay's Bluff looking towards the W and showing the two rock bodies composing Unit 1. From bottom to top, note modern intertidal notch, fossil terrace at +2.5 m above msl, and karstified eolianites characterized by steep, landward-dipping foresets; person for scale is 1.58 m tall. b) Thin-section view of sample CRO 16 collected from the base of the lower rock body at McKay's Bluff. Note altered bioclasts and early rim cement (arrow).

| Sample # | Locality      | Unit | <sup>87</sup> Sr/ <sup>86</sup> Sr | Std      | Age (Ma) |
|----------|---------------|------|------------------------------------|----------|----------|
| CRO 17   | McKays' Bluff | 2    | 0.709156                           | 0.000006 | 0.4-0.8  |
| CRO 18   | McKays' Bluff | 2    | 0.709174                           | 0.000006 | 0.0-0.3  |
| CRO 20   | McKays' Bluff | 2    | 0.709147                           | 0.000006 | 0.6-1.0  |
| CRO 21   | McKays' Bluff | 2    | 0.709146                           | 0.000006 | 0.6-1.0  |

Table 3. Sr-isotope data obtained in this study. Std = standard deviation.

#### The Bullet Hill Road Cut

The Bullet Hill road cut (N22°44.184', W74°05.159'; Figures 9 and 10) is one of the most

spectacular outcrops on Crooked Island, along with McKay's Bluff, and it exposes geological features that have so far never been observed elsewhere in the Bahamas. Bullet Hill is a 5 km long, 35 m high, NW-SE trending ridge located in the eastern part of the island (Figure 3). It is located about 1 km from the northern coastline and 2 km from the bank edge. The western portion of the ridge is marked by a depression that is cross cut by the single paved road on the island. The road cut has been precisely surveyed at the elevation of 33 feet (10.06 m), and it exposes the anatomy of the Bullet Hill ridge on both of its sides over a horizontal distance of about 300 m and a height of up to 5 m.

The Bullet Hill ridge is a composite ridge. However, unlike other complex ridges that display vertically stacked carbonate bodies with intervening subhorizontal paleosols (e.g., the Collins Avenue exposure in New Providence; Hearty and Kindler, 1997; Reid, 2010), this one consists of two sedimentary units separated by a subvertical to oblique boundary. The older unit, on the landward (SW) side of the ridge, consists of a fine-grained oolite (Figure 11a) showing high-angle foresets dipping toward the SW, and exhibits rhizoliths. The younger unit, on the seaward (NE) side of the ridge, is made of a coarser-grained oolitic calcarenite with scattered bioclasts and lithoclasts. It is characterized by fenestrae-rich, low-angle planar cross beds dipping toward the NE (i.e., toward the sea). In thin section, these rocks further show an early generation of fibrous rim cement and a late phase of blocky sparite (Figure 11b). On the western wall of the road cut, the boundary between the two units appears as an erosional surface steeply dipping toward the NE, and overlain by ca. 10 cm-size blocks derived from the older unit (Figure 9). On the eastern wall, the erosional surface shows a 3 m-long flat portion, at about +1 m above road level, and a notch with a prominent roof and a vertex situated at +0.5 m above road level (Figure 10). Amino-acid ratios obtained from the ridge average 0.434

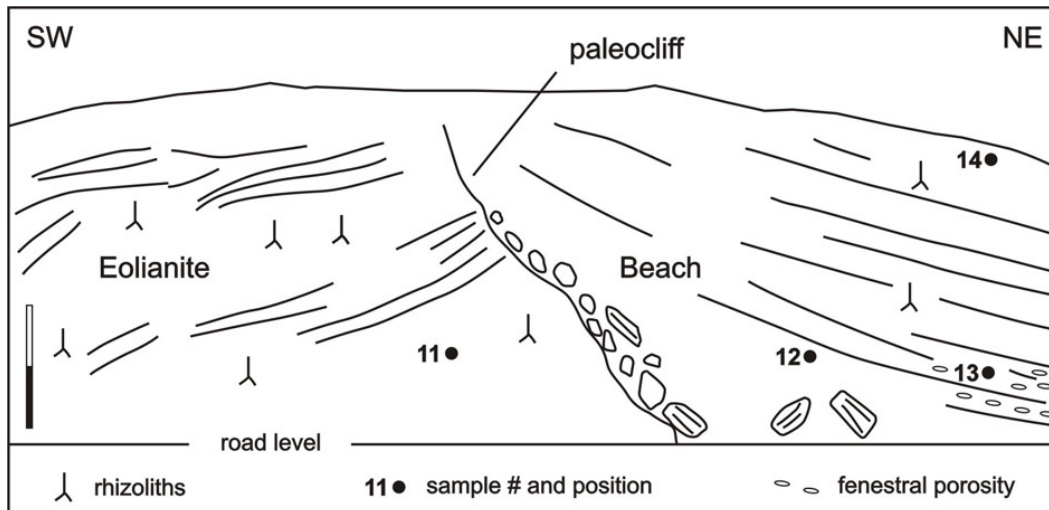


Figure 9. Rough sketch of the critical portion of the western wall of the Bullet Hill road cut showing cliffed eolianite and offlapping beach deposits. Vertical black and white bar = 2 m; horizontal extension of sketched exposure is about 20 m.

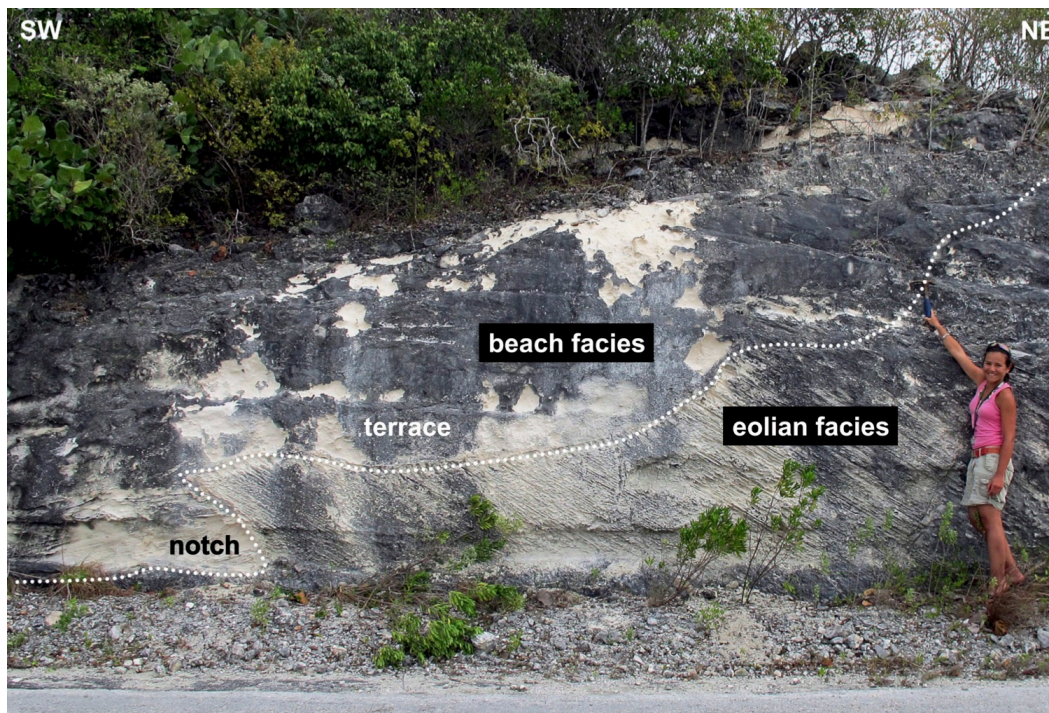


Figure 10. Partial view of the eastern wall of the Bullet Hill road cut showing the fossil notch and wave-cut terrace carved in Unit 3b eolianite and entombed by Unit 3b beach deposits. Note typical, steep (about 35°), landward-dipping foresets in eolian facies. Person for scale is 1.58 m tall.

( $n = 3$ ; Table 2), and there is no significant difference in A/I values between the two rock bodies composing the exposure. These sedimentological, petrographic, and geochronological data show that the two rock bodies composing the Bullet Hill ridge represent,

respectively, the eolian and the beach facies of Subunit 3b, correlated with the French Bay Member of the Grotto Beach Formation. Both of them were thus deposited during the last interglacial period, MIS 5e.

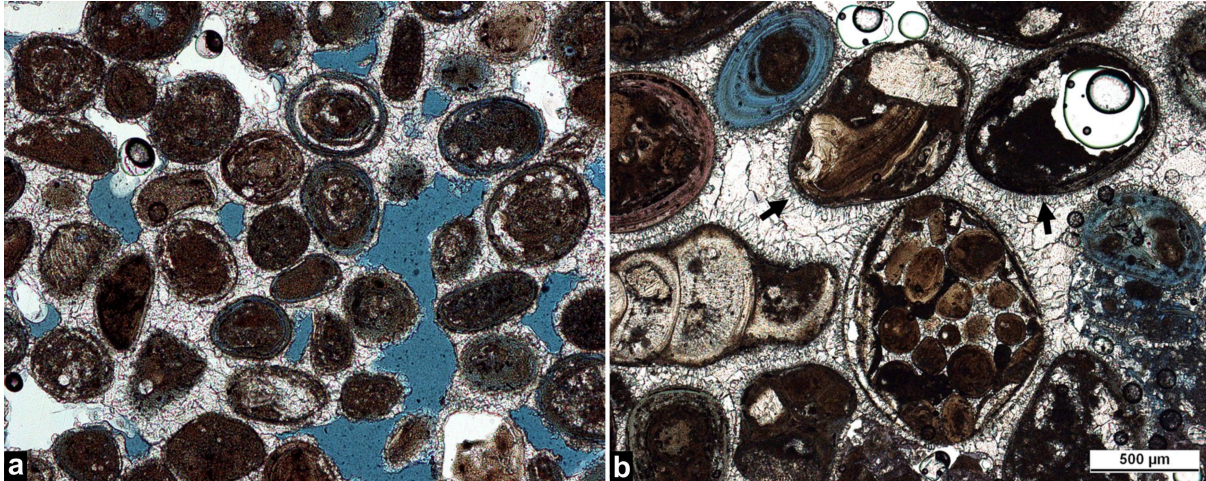


Figure 11. Comparative microscopic views of samples collected from the eolian and, respectively, the beach facies at the Bullet Hill road cut. a) Microfacies of sample CRO 10 collected from Unit 3b eolianite. Note good sorting, preserved intergranular porosity, fine grain size, and predominance of ooids. b) Microfacies of sample CRO 13 collected from Unit 3b beach facies. Note coarse grain size, presence of bioclasts and of an oolite lithoclast likely derived from Unit 3b eolianite, and extensive cementation. Note in particular the early generation of fibrous rim cement (arrows) preserved around most grains, indicating that early diagenesis took place in a marine setting. Scale applies to both photographs.

## DISCUSSION

### *Island Stratigraphy*

The stratigraphy of Crooked Island shows both similarities and differences with that derived from investigations on other islands of the Bahamas archipelago. The similarities include the occurrence of geological formations that have been described elsewhere in the Bahamas (Carew and Mylroie, 1995a; Kindler et al., 2010): the Pleistocene Grotto Beach Formation (Unit 3), which is very extensive as is also the case on the other islands (Carew and Mylroie, 1995a; Kindler and Hearty, 1997; Godefroid, 2012); and the Middle Pleistocene Owl's Hole Formation (Unit 2). The differences comprise the absence of geological formations that have been described elsewhere in the Bahamas. These formations, which might be discovered when Crooked is further explored, include the Middle Holocene North Point Member and the Late Pleistocene (MIS 5a) Whale Point Formation. The former is particularly well expressed on San Salvador (White and Curran, 1988), in the Exumas (Kindler,

1992), and on Long Island (Hearty, 2010), but is also missing from Mayaguana (Godefroid, 2012) and Great Inagua. Originally defined on San Salvador as the Almgreen Cay Formation (Hearty and Kindler, 1993), the latter is well identified on Eleuthera (Kindler and Hearty, 1995; Hearty, 1998), but has also been observed on Great Abaco, Bimini, and New Providence (Kindler and Hearty, 1996; Hearty and Kindler, 1997).

Differences also include the presence of rock bodies that are unique to Crooked Island, namely the cliffs of McKay's Bluff (Unit 1; Figure 8). As mentioned above, they mostly consist of highly weathered and karstified bioclastic eolianites underlain by marine facies of similar petrographic composition. Both amino-acid and Sr-isotope data suggest a Middle to Early Pleistocene age between 0.6 and 1 Ma for these deposits, which show similarities with both the Owl's Hole Formation (OHF; Carew and Mylroie, 1985, 1995a) and the Misery Point Formation (MPF; Godefroid, 2012). Indeed, Unit 1 has the same exclusively bioclastic composition as the MPF, but differs from the OHF, which may

contain oolitic/peloidal grainstone (Kindler and Hearty, 1996; Hearty, 2010). By contrast, as the OHF, (Kindler and Hearty, 1996; Hearty et al., 1999), Unit 1 comprises both eolian and marine facies, whereas the MPF is solely characterized by marine deposits (Godefroid, 2012). Unit 1 has further yielded anomalously low A/I ratios (Table 2), due to the partial leaching of amino acids, that are comparable to some values obtained from both the OHF (Hearty, 2010; Kindler, unpublished data) and the MPF (Godefroid, 2012). In contrast, the value of Sr-isotope ratios (around 0.709147; Table 3) produced by Unit 1, is closer to those measured from the OHF (0.709155) than those from the MPF (<0.709138) on Mayaguana (Kindler et al., 2011; Godefroid, 2012).

To reconcile all these observations, we propose that the upper rock body at McKay's Bluff represents the lowermost portion of the OHF, and that the lower one, which partly consists of marine deposits and must be older than 1 Ma, can be correlated with the youngest part of the Misery Point Formation. The marked paleosol separating the two units at about +5 m above msl could then possibly correspond to the boundary between the Early and the Middle Pleistocene. The presence of such old rocks at the surface of the island shows that, like Mayaguana (Godefroid, 2012), Crooked has been affected by minimal subsidence in the Quaternary.

#### *MIS 5e Sea Level*

It is not the aim of this paper to reconstruct the sea-level history during the last interglacial period. However, based on observations made at the Bullet Hill road cut, we can provide constraints to this history that will probably be useful for future researchers.

The occurrence of two laterally juxtaposed rock bodies of MIS 5e age separated by an erosional surface at the Bullet Hill outcrop (Figures 9 and 10) confirms the previous assertions of numerous authors (e.g., Aahron et al., 1980; Hearty and Kindler, 1993; Hearty et al.

2007, Thompson et al., 2011) regarding the occurrence of high-frequency (i.e., "sub-Milankovitch") sea-level fluctuations during the last interglacial. Nonetheless, the presence of a fossil intertidal notch carved in and filled by MIS 5e deposits at +11 m above msl (Figure 10) shows that, during one of these fluctuations, sea level probably reached an elevation about 5 m higher than previous estimates (e.g., +6 m, Hearty et al., 2007; Blanchon et al., 2009). Definitely, the elevation of these features (notch and marine deposits) cannot be explained by an uplift of the island, because coral-reef terraces of last-interglacial age are found at about the same elevation on Crooked as on all other Bahamian islands (i.e., seldom more than +2 m; Neumann and Hearty, 1996; Figure 5). Further, as indicated by the relatively elevated A/I values measured on this exposure and also by the fairly large volume of marine deposits overlying the erosional surface, this peak highstand was probably reached quite early in the MIS 5e interglacial rather than at the end of this period, as previously suggested (Neumann and Hearty, 1996; Hearty et al., 2007). Finally, the depositional environments of the two rock bodies exposed on either side of the erosional surface at the Bullet Hill road cut (eolian versus intertidal) do not provide evidence for a mid-5e regression (Hearty et al., 2007; Thompson et al., 2011), but rather for a simple sea-level rise from a lower elevation as advocated by Blanchon et al. (2009) and Godefroid (2012).

#### *Island Accretion*

Our geological map of Crooked (Figure 3) shows that the oldest stratigraphic units (# 1 and 2; MPF and OHF) are only exposed along the northern coastline, and that unit age generally decreases from N to S. Such an occurrence is uncommon for carbonate islands and, to our knowledge, has only been observed on Mayaguana. Most islands, such as Bermuda (Vacher et al., 1995), New Providence (Garrett and Gould, 1984; Hearty and Kindler, 1997) and

San Salvador (Kindler and Hearty, 1993) comprise a central core of weathered rocks surrounded by younger stratigraphic units (e.g., “Older Bermuda” and “Younger Bermuda”; Vacher, 1973). Two alternative explanations can be proposed to account for this asymmetrical distribution on Crooked: (1) island accretion occurred under the influence of a strong environmental gradient (e.g., predominant wind or current direction), or (2) the northern margin of the Crooked-Acklins platform experienced a major collapse in the recent past. We tend to favour the second hypothesis because of the alignment of this margin with that of the Mayaguana bank (Figure 1) where a similar asymmetrical distribution of stratigraphic units has been observed. Both banks could have collapsed due to renewed tectonic activity along a fault line. However, a preliminary modelling experiment suggests that the failure did not cause an uplift of Crooked Island, because this would imply anomalously small values of flexural rigidity ( $10^{19}$  Nm) to explain such short wavelength deformation (Simpson, personal communication 2014).

### CONCLUSIONS

Our preliminary geological investigations on Crooked Island show that, with a few exceptions (North Point Member, Whale Point Formation), it comprises stratigraphic units that

are also present on other Bahamian islands (Hanna Bay Member, Grotto Beach, Owl’s Hole and Misery Point formations). Of particular interest are the impressive McKay’s Bluff cliffs that appear to expose the basal portion of the Owl’s Hole Formation and the upper part of the Misery Point Formation that has so far only been observed on Mayaguana. The MIS 5e record is remarkable. In particular, beach deposits and an intertidal notch at +11 m above msl strongly suggest that sea-level peaked at a much higher elevation than previously assessed, implying pronounced melting of polar ice. No doubt, future research on Crooked and neighbouring Acklins Island will lead to exciting new geological discoveries.

### ACKNOWLEDGMENTS

We thank F. Gischig (University of Geneva) for thin-section manufacturing, D.S. Kaufman and J. Bright (Northern Arizona University) for providing the amino-acid racemization data, and M. Chiaradia (University of Geneva) for Sr-isotope analyses. B. Glumac and J.L. Carew gave constructive comments on a previous version of this paper. Many thanks to D. and B. Ferguson for their hospitality on Crooked Island. This research was supported by the Swiss National Science Foundation (grant #200020-124608/1).

### REFERENCES

- Aharon, P., Chappell, J., and Compston, W., 1980, Stable isotope and sea-level data from New Guinea supports Antarctic ice-surge theory of ice ages: *Nature*, v. 283, p. 649-651.
- Blanchon P., Eisenhauer A., Fietzke J., Liebetrau V., 2009, Rapid sea-level rise and reef back-stepping at the close of the last interglacial highstand: *Nature*, v. 458, p. 881-884.
- Caputo, M.V., 1995, Sedimentary architecture of Pleistocene eolian calcarenites, San Salvador Island, Bahamas, *in* Curran, H.A. and White, B., eds., *Terrestrial and shallow marine geology of the Bahamas and Bermuda: Geological Society of America Special Paper*, v. 300, p. 63-76.
- Carew, J.L., and Mylroie, J.E., 1985, The Pleistocene and Holocene stratigraphy of San Salvador Island, Bahamas, with reference to marine and terrestrial lithofacies at French Bay, *in* Curran, H.A., ed., *Pleistocene and Holocene carbonate environments on San Salvador Island, Bahamas: Geological Society of America, Annual meeting guidebook*, Ft. Lauderdale, FL, CCFL Bahamian Field Station, p. 11-61.
- Carew, J.L., and Mylroie, J.E., 1995a, Depositional model and stratigraphy for the Quaternary geology of

- the Bahama Islands, in Curran, H.A. and White, B., eds., *Terrestrial and shallow marine geology of the Bahamas and Bermuda: Geological Society of America Special Paper*, v. 300, p. 5-32.
- Carew, J.L., and Mylroie, J.E., 1995b, Quaternary tectonic stability of the Bahamian archipelago: evidence from fossil coral reefs and flank margin caves: *Quaternary Science Reviews*, v. 14, p. 145-153.
- Chen, J.H., Curran, H.A., White, B., and Wasserburg, G.J., 1991, Precise chronology of the last interglacial period:  $^{234}\text{U}$ - $^{230}\text{Th}$  data from fossil coral reefs in the Bahamas: *Geological Society of America Bulletin*, v. 103, p. 82-97.
- Cotilla Rodriguez, M.O., Franzke, H.J., and Cordoba Barba, D., 2007, Seismicity and seismoactive faults of Cuba: *Russian Geology and Geophysics*, v. 48, p. 505-522.
- Garrett, P., and Gould, S.J., 1984, *Geology of New Providence Island, Bahamas: Geological Society of America Bulletin*, v. 95, p. 209-220.
- Godefroid, F., 2012, Géologie de Mayaguana, SE de l'archipel des Bahamas: *Terre & Environnement*, v. 108, 230 p.
- Gradstein, F.M., Ogg, J.G., Smith, A.G., Bleeker, W., and Lourens, L.J., 2004, A new geologic time scale with special reference to Precambrian and Neogene: *Episodes*, v. 27, p. 83-100.
- Hearty, P.J., 1998, The geology of Eleuthera Island, Bahamas: a rosetta stone of Quaternary stratigraphy and sea-level history: *Quaternary Science Reviews*, v. 17, p. 333-355.
- Hearty, P., 2010, Chronostratigraphy and morphological changes in *Cerion* land snail shells over the past 130 ka on Long Island, Bahamas: *Quaternary Geochronology*, v. 5, p. 50-64.
- Hearty P.J., and Kaufman, D.S., 2000, Whole-rock aminostratigraphy and Quaternary sea-level history of the Bahamas: *Quaternary Research*, v. 54, p. 163-173.
- Hearty P.J., and Kaufman, D.S., 2009, A *Cerion*-based chronostratigraphy and age model from the Central Bahama Islands: amino-acid racemization and  $^{14}\text{C}$  in land snails and sediments: *Quaternary Geochronology*, v. 4, p. 148-159.
- Hearty, P.J., and Kindler, P., 1993, New perspectives on Bahamian geology: San Salvador Island, Bahamas: *Journal of Coastal Research*, v. 9, p. 577-594.
- Hearty, P.J., and Kindler, P., 1997, The stratigraphy and surficial geology of New Providence and surrounding islands, Bahamas: *Journal of Coastal Research*, v. 13, p. 798-812.
- Hearty P.J., Hollin J.T., Neumann A.C., O'Leary, M.J., and McCulloch M., 2007, Global sea-level fluctuations during the Last Interglaciatiion (MIS 5e): *Quaternary Science Reviews*, v. 26, p. 2090-2112.
- Hearty, P.J., Kindler, P., Cheng, H., and Edwards, L., 1999, A +20 m middle Pleistocene sea-level highstand (Bermuda and The Bahamas) due to partial collapse of Antarctic ice: *Geology*, v. 27, p. 375-378.
- Hearty, P.J., Vacher, H.L., and Mitterer, R.M., 1992, Aminostratigraphy and ages of Pleistocene limestones of Bermuda: *Geological Society of America Bulletin*, v. 104, p. 471-480.
- Horwitz, E.P., Chiarizia, R., and Dietz, M.L., 1992, A novel strontium-selective extraction chromatographic resin: *Solvent Extraction and Ion Exchange*, v. 10, p. 313-336.
- Howarth R.J., and McArthur, J.M., 1997, Statistics for strontium isotope stratigraphy. A robust LOWESS fit to the marine Sr-isotope curve for 0 - 206 Ma, with look-up table for the derivation of numerical age: *Journal of Geology*, v. 105, p. 441-456.
- Kindler, P., 1992, Coastal response to the Holocene transgression in the Bahamas: episodic sedimentation versus continuous sea-level rise: *Sedimentary Geology*, v. 80, p. 319-329.
- Kindler, P., and Hearty, P.J., 1995, Pre-Sangamonian eolianites in the Bahamas? New evidence from Eleuthera Island: *Marine Geology*, v. 127, p. 73-86.
- Kindler, P., and Hearty, P.J., 1996, Carbonate petrography as an indicator of climate and sea-level changes: new data from Bahamian Quaternary units: *Sedimentology*, v. 43, p. 381-399.
- Kindler, P., and Hearty, P.J., 1997, *Geology of The Bahamas: architecture of Bahamian Islands*, in Vacher, H.L. and Quinn, T.M., eds., *Geology and hydrogeology of carbonate islands: Developments in Sedimentology*, v. 54, Elsevier, Amsterdam, p. 141-160.

- Kindler, P., and Hine, A.C., 2009, The paradoxical occurrence of oolitic limestone on the eastern islands of Great Bahama Bank: where do the ooids come from?, *in* Swart, P.K., Eberli, G.P. and McKenzie, J.A., eds., *Perspectives in carbonate geology. A tribute to the career of Robert Nathan Ginsburg*: IAS Special Publication, n° 41, p. 113-122.
- Kindler, P., Godefroid, F., Chiaradia, M., Ehlert, C., Eisenhauer, A., Frank, M., Hasler, C.-A., and Samankassou, E., 2011, Discovery of Miocene to early Pleistocene deposits on Mayaguana, Bahamas: evidence for recent active tectonism on the North American margin: *Geology*, v. 39, p. 523-526.
- Kindler P., Mylroie J.E., Curran, H.A., Carew, J.L., Gamble, D.W., Rothfus, T.A., Savarese, M., and Sealey, N.E., 2010, *Geology of Central Eleuthera, Bahamas: A Field Trip Guide*: San Salvador, Bahamas, Gerace Research Centre, 74 p.
- Lynts, G.W., 1970, Conceptual model of the Bahamian platform for the last 135 million years: *Nature*, v. 225, p. 1226-1228.
- McArthur J.M., Howarth R.J., and Bailey T.R., 2001, Strontium isotope stratigraphy: LOWESS Version 3. Best-fit line to the marine Sr-isotope curve for 0 to 509 Ma and accompanying look-up table for deriving numerical age: *Journal of Geology*, v. 109, p. 155-169.
- Neumann, A.C., and Hearty, P.J., 1996, Rapid sea-level changes at the close of the last interglacial (substage 5e) recorded in Bahamian island geology: *Geology*, v. 24, p. 775-778.
- Pierson, B.J., 1982, Cyclic sedimentation, limestone diagenesis and dolomitization in upper Cenozoic carbonates of the southeastern Bahamas: Unpublished Ph.D. thesis, University of Miami, Florida, USA, 286 p.
- Rankey, E.C., and Reeder, S.L., 2010, Controls on platform-scale patterns of surface sediments, shallow Holocene platforms, Bahamas: *Sedimentology*, v. 57, p. 1545-1565.
- Reid, S.B., 2010, The complex architecture of New Providence Island (Bahamas) built by multiple Pleistocene sea level highstands: Unpublished M.Sc. thesis, University of Miami, Florida, [http://scholarlyrepository.miami.edu/oa\\_thesis/77](http://scholarlyrepository.miami.edu/oa_thesis/77), 199 p.
- Savarese, M., and Hoeflein, F.J., 2012, Sea level and the paleoenvironmental interpretation of the Middle to Late Holocene Hanna Bay Limestone, San Salvador, Bahamas: a high foreshore setting without a higher-than-present eustatic highstand, *in* Gamble, D.G. and Kindler, P., eds., *Proceedings of the 15<sup>th</sup> Symposium on the Geology of the Bahamas and other carbonate regions*: Gerace Research Center, San Salvador, Bahamas, p. 161-181.
- Sealey, N.E., 2006, *Bahamian Landscapes. An introduction to the geology and physical geography of the Bahamas*: Macmillan Publishers, Oxford, UK, 174 p.
- Thompson, W.G., Curran, H.A., Wilson, M.A., and White, B., 2011, Sea-level oscillations during the last interglacial highstand recorded by Bahamas corals: *Nature Geoscience*, v. 4, p. 684-687.
- Vacher, L., 1973, Coastal dunes of Younger Bermuda, *in* Coates, D.R., ed., *Coastal geomorphology. Publications in Geomorphology*: State University of New York, p. 355-391.
- Vacher, H.L., Hearty, P.J., and Rowe, M.P., 1995, Stratigraphy of Bermuda: nomenclature, concepts and status of multiple systems of classification, *in* Curran, H.A. and White, B., eds., *Terrestrial and shallow marine geology of the Bahamas and Bermuda*: Geological Society of America Special Paper, v. 300, p. 271-294.
- White, B., and Curran, H.A., 1988, Mesoscale physical sedimentary structures and trace fossils in Holocene carbonate eolianites from San Salvador Island, Bahamas: *Sedimentary Geology*, v. 55, p. 163-184.